Conclusions

At turbulent jet excitation by high-intensity sound the sound wave form plays a substantial role not only in forming coherent structures in the jet but also in forming the jet structure itself. Sinusoidal excitation generates rather extended vortices in jets and can cause lateral jet oscillations. Sawtoothlike wave excitation leads to the formation of compact disturbances both in subsonic and supersonic jets. The intrinsic shock-wave formation of supersonic jets can be destroyed in this case and the disturbance movement along the jet boundary at supersonic convective velocity is accompanied by Mach wave radiation.

Acknowledgment

This work was supported by the Russian Fund of Fundamental Investigations (Grant 03-01-00492).

References

[1]Ginevsky, A. S., Vlasov, Y. V., and Karavosov, R. K., *Acoustic Control of Turbulent Jets,* Physmathlit, Moscow, 2001 (in Russian).

[2]Sokolov, M., Kleis, S. J., and Hussain, A. K. M. F., "Coherent Structures Induced by Two Simultaneous Sparks in Axisymmetric Jet," *AIAA Journal*, Vol. 19, No. 8, 1981, pp. 1000–1008.

[3]Vlasov, Ye. V., Ginevsky, A. S., Karavosov, R. K., and Makarenko, T. M., "Effect of Non-Harmonic Signal on Turbulent Jet," *Inzhenerno-Fizicheskii Zhurnal*, Vol. 74, No. 5, 2001, pp. 33–35 (in Russian).

[4]Pimshtein, V. G., "Disturbance Generation in Supersonic Jets Under Acoustic Excitation," *AIAA Journal*, Vol. 32, No. 7, 1994, pp. 1345–1349.

W. J. Devenport
Associate Editor

Optimal Disturbances in Boundary Layers Subject to Streamwise Pressure Gradient

Anatoli Tumin*
University of Arizona, Tucson, Arizona 85721
and
David E. Ashpis†
NASA John H. Glenn Research Center at Lewis Field, Cleveland, Ohio 44135

Introduction

LAMINAR–TURBULENT transition in shear flows is still an enigma in the area of fluid mechanics. The conventional explanation of the phenomenon is based on the instability of the shear flow with respect to infinitesimal disturbances. The conventional hydrodynamic stability theory deals with the analysis of normal modes that might be unstable. The latter circumstance is accompanied by an exponential growth of the disturbances that might lead to laminar–turbulent transition. Nevertheless, in many cases, the transition scenario bypasses the exponential growth stage associated with the normal modes. This type of transition is called *bypass transition.* An understanding of the phenomenon has eluded us to this day. One possibility is that bypass transition is associated with so-called algebraic (nonmodal) growth of disturbances in shear flows.[1,2]

A numerical analysis of spatial nonmodal growth within the scope of the linearized boundary-layer equations for an incompressible flow over a flat plate was carried out in Refs. 3 and 4. Spatial analysis within the scope of the linearized Navier–Stokes equations (quasi-parallel approximation of compressible and incompressible flows) was presented in Refs. 5–7. Recently, the method of Ref. 4 was generalized for the case of compressible boundary layers.[8] The main results of these theoretical models are as follows: 1) A system of counter-rotating streamwise vortices, which are periodic in the spanwise direction, provides the strongest growth of the disturbance. 2) There is an optimal spacing of the streamwise vortices, which leads to the strongest effect.

The effect of pressure gradients on the transient growth mechanism was considered within the scope of temporal theory by Corbett and Bottaro[9] and within the scope of spatial theory by Tumin and Reshotko.[7] Both studies were based on the quasi-parallel flow assumption. Tumin[10] analyzed the pressure-gradient effect for the Falkner–Skan profile within the scope of an analytical model when the spanwise wave number is very small. The pressure-gradient effect within the scope of spatial theory with nonparallel base flow and finite spanwise wave numbers has not yet been considered.

Another motivation for the present work stems from separation flow control on low-pressure turbines (LPTs). The performance of LPTs is strongly affected by the flow separation. There is a possibility of delaying the boundary-layer separation by tripping the boundary layer with the help of roughness elements or other devices. Usually, a trial-and-error method is used to determine an appropriate placement of the control elements. This approach is time consuming and expensive. A recent investigation by Reshotko and Tumin[11] demonstrated that roughness-induced transition might be related to the transient growth mechanism.

Periodically spaced in the spanwise direction, roughness elements generate a system of counter-rotating streamwise vortices. Due to a secondary instability mechanism, the streamwise vortices can lead to earlier transition to turbulence. They also provide a mixing enhancement due to redistribution of the streamwise momentum. Consequently, optimization of the streamwise vortices for maximum energy growth leads to maximization of the flow control effectiveness. In the present work, an analysis of the optimal disturbances/streamwise vortices associated with the transient growth mechanism is performed for boundary layers in the presence of a streamwise pressure gradient. The theory will provide the optimal spacing of the control elements in the spanwise direction and their placement in the streamwise direction.

Governing Equations

Because the flows of interest have relatively low Mach numbers, we consider steady three-dimensional disturbances in an incompressible two-dimensional boundary layer. We choose the streamwise coordinate x along the surface. The coordinate y will measure distance from the wall. We define a small parameter $\varepsilon = \sqrt{(\nu/U_{\text{ref}}L_{\text{ref}})}$ that is the inverse square root of the Reynolds number, and ν, U_{ref}, and L_{ref} are viscosity, reference velocity, and reference length, respectively. The streamwise coordinate is scaled with L_{ref} while the vertical coordinate y and spanwise coordinate z are scaled with $\sqrt{(\nu L_{\text{ref}}/U_{\text{ref}})}$. The following scaling is assumed for the velocity disturbances u, v, and w and the pressure p:

$$u \sim U_{\text{ref}}, \qquad v \sim \varepsilon U_{\text{ref}}, \qquad w \sim \varepsilon U_{\text{ref}}, \qquad p \sim \varepsilon^2 \rho U_{\text{ref}} \quad (1)$$

This scaling of the linearized Navier–Stokes equations and neglecting the curvature effects lead to the governing equations for Görtler instability, with the Görtler number equal to zero. We look for a periodic solution in the spanwise direction, with the corresponding wave number β. The governing equations for

Received 21 February 2003; presented as Paper 2003-4242 at the AIAA 33rd Fluid Dynamics Conference, Orlando, FL, 23–26 June 2003; revision received 1 August 2003; accepted for publication 4 August 2003. This material is declared a work of the U.S. Government and is not subject to copyright protection in the United States. Copies of this paper may be made for personal or internal use, on condition that the copier pay the $10.00 per-copy fee to the Copyright Clearance Center, Inc., 222 Rosewood Drive, Danvers, MA 01923; include the code 0001-1452/03 $10.00 in correspondence with the CCC.

*Associate Professor, Department of Aerospace and Mechanical Engineering; tumin@email.arizona.edu. Senior Member AIAA.

†Aerospace Engineer. Senior Member AIAA.

the amplitude functions can be written in dimensionless form as follows[3,4]:

$$\frac{\partial u}{\partial x} + \frac{\partial v}{\partial y} + \beta w = 0 \tag{2}$$

$$\frac{\partial}{\partial x}(Uu) + V\frac{\partial u}{\partial y} + v\frac{\partial U}{\partial y} = \frac{\partial^2 u}{\partial y^2} - \beta^2 u \tag{3}$$

$$\frac{\partial}{\partial x}(uV + vU) + \frac{\partial}{\partial y}(2Vv) + \beta V w + \frac{\partial p}{\partial y} = \frac{\partial^2 v}{\partial y^2} - \beta^2 v \tag{4}$$

$$\frac{\partial}{\partial x}(Uw) + \frac{\partial}{\partial y}(Vw) - \beta p = \frac{\partial^2 w}{\partial y^2} - \beta^2 w \tag{5}$$

where $U(x, y)$ and $V(x, y)$ are the streamwise and normal velocity components of the base flow, respectively. The streamwise velocity $U(x, y)$ is scaled with U_{ref}, and the normal velocity $V(x, y)$ is scaled with $\varepsilon U_{\text{ref}}$.

The following boundary conditions are applied to the solutions:

$$y = 0: \qquad u = v = w = 0 \tag{6a}$$

$$y \to \infty: \qquad u, w, p \to 0 \tag{6b}$$

Equations (2–5) can be solved subject to boundary conditions (6a) and (6b) with prescribed initial velocity perturbations at $x = x_0$.

Optimization of Energy Growth

The authors of Refs. 3 and 4 employed an iterative procedure to find the optimal disturbances in terms of the maximum of the energy growth ratio $G = E_{\text{out}}/E_{\text{in}}$, where E_{in} and E_{out} stand for the input and output energy norms. Andersson et al.[3] used the same definitions of E_{in} and E_{out} as for the disturbance energy,

$$E = \int_0^{y_{\max}} (u^2 + \varepsilon^2 v^2 + \varepsilon^2 w^2)\,\mathrm{d}y \tag{7}$$

whereas Luchini[4] employed the knowledge that the optimal disturbances are represented by streamwise vortices with corresponding output as streamwise velocity streaks:

$$E_{\text{in}} = \varepsilon^2 \int_0^{y_{\max}} (v^2 + w^2)\,\mathrm{d}y \tag{8a}$$

$$E_{\text{out}} = \int_0^{y_{\max}} u^2\,\mathrm{d}y \tag{8b}$$

$$G = \frac{E_{\text{out}}}{E_{\text{in}}} = \varepsilon^{-2}\frac{\int_0^{y_{\max}} u^2\,\mathrm{d}y}{\int_0^{y_{\max}} (v^2 + w^2)\,\mathrm{d}y} \tag{8c}$$

As was shown in Ref. 3, the two definitions of the optimal disturbances lead to the same results at Reynolds numbers of 10^4 and higher. Because the iteration procedure based on the optimization of ratio (8c) provides significant simplification, we adopt it for the following analysis. Because Eqs. (2–5) are independent of ε, the value of $\varepsilon^2 G$ is invariant with respect to the Reynolds number.

Numerical Results

Falkner–Skan Base Flow

We consider a Falkner–Skan family of boundary-layer profiles with freestream velocity distribution $U_e = Cx^m$ and corresponding Hartree parameter $\beta_H = 2m/(m+1)$. For the purpose of convenience, we have used the velocity scale $U_{\text{ref}} = U_{eL} = CL^m$ and the length scale $L_{\text{ref}} = L/(m+1)$. The latter allowed the use of the conventional scaling of boundary-layer solutions with $H_{\text{ref}} = \sqrt{[\nu L/(m+1)U_{eL}]} = \sqrt{(\nu L_{\text{ref}}/U_{\text{ref}})}$.

Figure 1 shows the scaled energy ratio vs spanwise wave number β for three Hartree parameters, $\beta_H = -0.1, 0.0$, and 0.1. The starting and the ending points, x_{in}/L and x_{out}/L, are equal to 0.2 and 1.0, respectively. The Reynolds number Re_L in Fig. 1 and what follows is defined as $U_{eL}L/\nu$. One can see that an unfavorable pressure gradient ($\beta_H < 0$) leads to an increase in the energy growth, whereas a favorable pressure gradient ($\beta_H > 0$) leads to suppression of the transient growth mechanism. The latter is consistent with results obtained within the scope of parallel flow approximation.[7] Analysis of various starting points, x_{in}/L, has shown that, in addition to an optimal spacing between perturbers, there is an optimal location from the leading edge. (A similar result was observed in Ref. 8 for compressible boundary layers over a flat plate.)

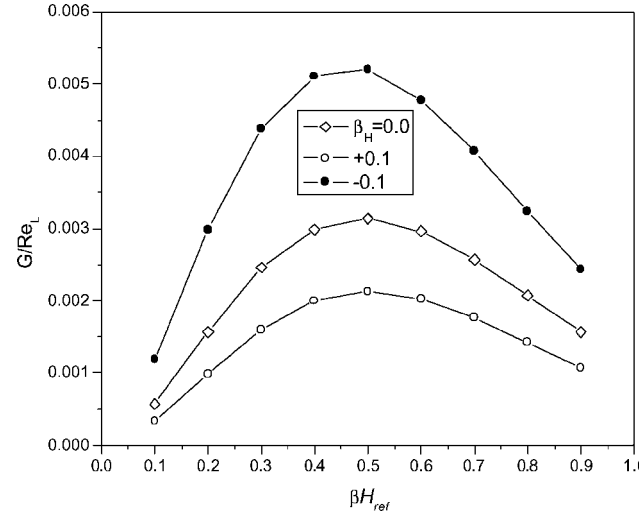

Fig. 1 Effects of the spanwise wave number β and the Hartree parameter β_H on transient growth (starting point $x_{\text{in}}/L = 0.2$).

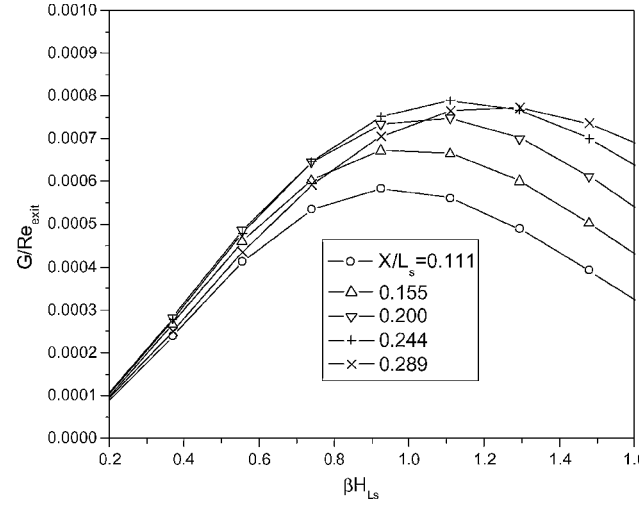

Fig. 2 Effects of the spanwise wave number β and the starting point x_{in}/L on transient growth at the same conditions as the experiment in Ref. 12 ($\beta_H = 0.353$, $x_{\text{out}}/L_s = 0.444$).

Example of Low-Pressure Turbine Conditions

Volino[12] simulated LPT airfoil conditions in a low-speed wind tunnel. The test section was designed as a passage between two airfoils. The local freestream velocity at a favorable pressure-gradient region was closely approximated by the following equation:

$$U_e/U_{\text{exit}} = 1.48(x/L_s)^{0.214} \tag{9}$$

where L_s is the suction surface length and U_{exit} is the nominal exit freestream velocity based on the inviscid solution. Distribution (9) corresponds to a Falkner–Skan flow with the Hartree parameter $\beta_H = 0.353$.

Figure 2 demonstrates the energy ratio scaled with the Reynolds number ($Re_{\text{exit}} = U_{\text{exit}}L_s/\nu$) vs the spanwise wave number scaled

with $H_{Ls} = \sqrt{\nu L_s / U_{\text{exit}}}$. The ending point was prescribed at $x_{\text{out}}/L_s = 0.444$ while the starting points varied from 0.111 to 0.289. One can see that there is an optimal starting point, x_{in}/L. The optimal velocity perturbation profiles at $x_{\text{out}}/L_s = 0.444$ (for u), $x_{\text{in}}/L_s = 0.111$ (for v and w), and $\beta H_{Ls} = 0.925$ are shown in Fig. 3.

The results indicate that we are dealing with a very strong favorable pressure gradient that suppresses the transient growth mechanism. For example, at a typical LPT cruise Reynolds number of 5×10^4, the transient growth will provide an energy amplification of less than 50. This is a relatively small number. If we take into account that, in practice, the perturber will not produce the optimal inflow field, the real amplification will be of an even smaller value. For example, in a Blasius boundary layer, the theory predicts amplification of 250 at the same Reynolds number of 5×10^4 (Ref. 9). Correlation between the transient growth factor and transition has not been established yet; therefore, the effectiveness of the transient growth mechanism in preventing flow separation cannot be assessed quantitatively at the present time.

There is a possibility of enhancing the transient growth mechanism by means of wall cooling. The effect of wall cooling was investigated by Tumin and Reshotko[7] within the scope of a parallel flow approximation. In order to estimate possible increases of the energy ratio on a cold wall at a high favorable pressure gradient, we utilize the method of Ref. 7 for a compressible flow with local Mach number of 0.5 and Hartree parameter of 0.353. The results are shown in Fig. 4. One can see that cooling of the wall might provide a tenfold increase in the energy ratio.

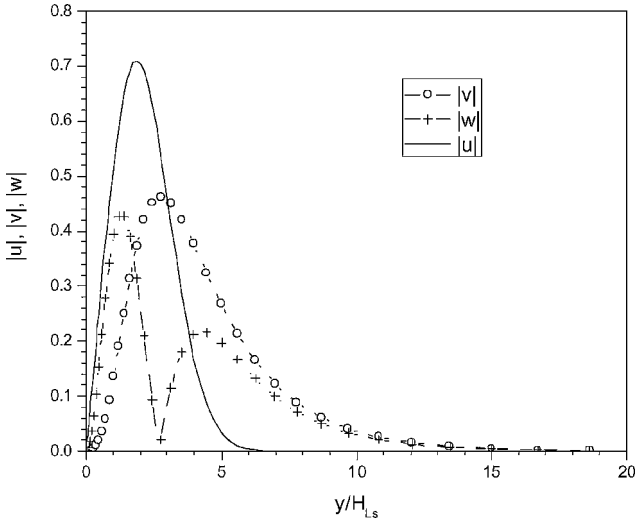

Fig. 3 The optimal velocity perturbation u at the ending point $x_{\text{out}}/L_s = 0.444$ and corresponding velocity profiles v and w at the starting point $x_{\text{in}}/L_s = 0.111$. The parameters correspond to the experimental conditions in Ref. 12 ($\beta H_{Ls} = 0.925$).

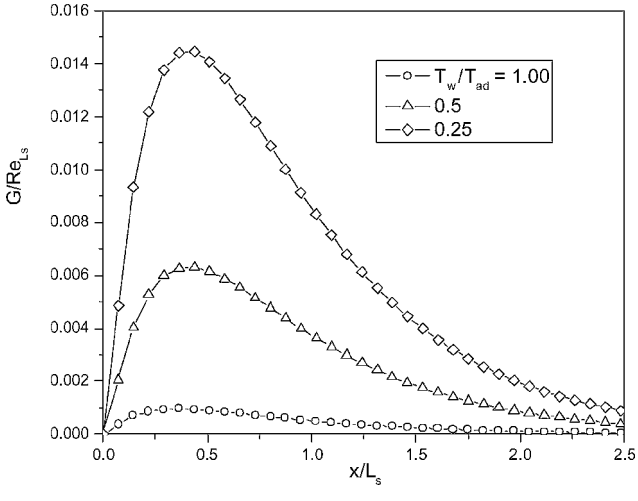

Fig. 4 Effect of the temperature factor on energy growth at the experimental conditions in Ref. 12.

Summary

The results for the transient growth phenomenon within the scope of the linearized boundary-layer equations in the presence of a streamwise pressure gradient are consistent with previous results obtained within the scope of the parallel flow approximation and linearized Navier–Stokes equations.[7] A favorable pressure gradient decreases the nonmodal growth while an unfavorable pressure gradient leads to an increase of the amplification.

The example of a Falkner–Skan flow with a Hartree parameter $\beta_H = 0.353$ corresponds to the experimental data[12] and simulates the flow over an LPT airfoil upstream of the separation point. At this pressure gradient, the transient growth mechanism is suppressed and the energy amplification at low Reynolds number has a small value. The theory of the transient growth mechanism predicts that it is possible to enhance the energy growth by means of wall cooling. The example within the scope of the parallel flow theory[7] demonstrates that cooling of the wall might provide a tenfold increase in the energy ratio. Future experiments on boundary-layer tripping accompanied by wall cooling will contribute to our understanding of the bypass transition mechanism.

The method also predicts that there is an optimal spacing between perturbers and an optimal location from the leading edge.

Consideration of the optimal velocity perturbations in Fig. 3 indicates that they are spreading across the boundary layer. This means that an array of generators localized on the wall will not provide excitation of the optimal disturbances. Therefore, the question of realizability of the optimal disturbances arises. For example, one can solve the receptivity problem for an array of generators on the wall and evaluate their shapes (or other parameters) to find the ones that provide disturbance profiles closest to the optimal ones. Another option is to solve the receptivity problem for distributed generators upstream of the starting point x_{in} and to find the distribution of generators that leads to the optimal disturbances. The next option is to design a disturbance generator that directly affects the flow inside the boundary layer instead of perturbing the near-wall region only. These fundamental issues should be addressed in future research programs on the application of bypass transition mechanisms to separation flow control at low Reynolds numbers.

Acknowledgments

The work has been partially supported by an Air Force Office of Scientific Research grant monitored by J. Schmisseur and partially by the NASA John H. Glenn Research Center under Cooperative Agreement NCC 3-991. The authors appreciate useful comments provided by Stewart Leib of the Ohio Aerospace Institute.

References

[1]Reshotko, E., "Transient Growth: A Factor in Bypass Transition," *Physics of Fluids*, Vol. 13, 2001, pp. 1067–1075.

[2]Schmid, P. J., and Hennigson, D. S., *Stability and Transition in Shear Flows*, Springer, New York, 2001.

[3]Andersson, P., Berggren, M., and Henningson, D., "Optimal Disturbances and Bypass Transition in Boundary Layers," *Physics of Fluids*, Vol. 11, 1999, pp. 134–150.

[4]Luchini, P., "Reynolds Number Independent Instability of the Boundary Layer over a Flat Surface, Part 2: Optimal Perturbations," *Journal of Fluid Mechanics*, Vol. 404, 2000, pp. 289–309.

[5]Reshotko, E., and Tumin, A., "The Blunt Body Paradox—A Case for Transient Growth," *Laminar-Turbulent Transition*, edited by H. F. Fasel and W. S. Saric, Springer, New York, 2000, pp. 403–408.

[6]Reshotko, E., and Tumin, A., "Spatial Theory of Optimal Disturbances in a Circular Pipe Flow," *Physics of Fluids*, Vol. 13, 2001, pp. 991–996.

[7]Tumin, A., and Reshotko, E., "Spatial Theory of Optimal Disturbances in Boundary Layers," *Physics of Fluids*, Vol. 13, 2001, pp. 2097–2104.

[8]Tumin, A., and Reshotko, E., "Optimal Disturbances in Compressible Boundary Layers," AIAA Paper 2003-0792, Jan. 2003.

[9]Corbett, P., and Bottaro, A., "Optimal Perturbations for Boundary Layers Subjected to Stream-Wise Pressure Gradient," *Physics of Fluids*, Vol. 12, 2000, pp. 120–130.

[10]Tumin, A., "A Model of Spatial Algebraic Growth in a Boundary Layer Subjected to a Streamwise Pressure Gradient," *Physics of Fluids*, Vol. 13, 2001, pp. 1521–1523.

[11]Reshotko, E., and Tumin, A., "Investigation of the Role of Transient Growth in Roughness-Induced Transition," AIAA Paper 2002-2850, June 2002.

[12]Volino, R. J., "Separated Flow Transition Under Simulated Low-Pressure Turbine Airfoil Conditions: Part 1—Mean Flow and Turbulence Statistics," *Proceedings of the ASME TURBO EXPO 2002* [CD-ROM], American Society of Mechanical Engineers, Paper GT-2002-30236, 2002.

A. Plotkin
Associate Editor

In Situ Calibration Uncertainty of Pressure-Sensitive Paint

Tianshu Liu*
NASA Langley Research Center, Hampton, Virginia 23681-2199
and
John P. Sullivan†
Purdue University, West Lafayette, Indiana 47906

Introduction

PRESSURE-SENSITIVE paint (PSP) is an optical sensor for measuring surface pressure distributions on wind-tunnel models.[1,2] Because of oxygen quenching of luminescence, the luminescent intensity I emitted from PSP is related to air pressure p by the linear Stern–Volmer relation over a certain range:

$$I_{\text{ref}}/I = A(T) + B(T)(p/p_{\text{ref}}) \tag{1}$$

where I_{ref} and p_{ref} are the reference luminescent intensity and pressure at a known temperature, respectively. The Stern–Volmer coefficients $A(T)$ and $B(T)$ are temperature dependent because temperature affects both nonradiative deactivation and oxygen diffusion in a polymer. In principle, a priori calibration of PSP in a pressure cell can be used for conversion from the luminescent intensity to pressure using Eq. (1). However, this approach often leads to a considerable systematic error because the surface temperature distribution is not known and the illumination change on surface due to model deformation cannot be corrected by image registration. The systematic error is also related to uncontrollable environmental testing factors. Therefore, in actual PSP measurements, experimental aerodynamicists calibrate PSP in situ by fitting (or correlating) the normalized luminescent intensity to pressure tap data at a number of distributed locations. In a sense, in situ PSP calibration eliminates the systematic error associated with the temperature effect and the illumination change by absorbing it into the overall fitting error. In situ PSP calibration uncertainty is not sufficiently discussed, although Sajben[3] and Liu et al.[4] have given a general uncertainty analysis of PSP. Recently, Kammeyer et al.[5,6] assessed the accuracy of The Boeing Company production PSP system by statistical analysis of comparison between PSP and pressure transducers over a large numbers of data points on a 1/12th-scale model of a Cessna Citation. Tests were run at several Mach numbers from 0.22 to 0.82, two Reynolds numbers of 4.5 and 8.3×10^6, and 14 angles of attack ranging from −4 to 10 deg. Kammeyer et al. found that in situ calibration error was a function of the angle of attack (AOA) and Mach number. It was also found that the histogram of the overall set of in situ PSP errors obtained at all of the Mach numbers and AOA exhibited a distinct non-Gaussian distribution. In this Note, we study in situ calibration uncertainty of PSP through a simulation of PSP measurements in subsonic Joukowsky airfoil flows where in situ calibration uncertainty is mainly attributed to the temperature effect of PSP and illumination change on surface due to model deformation. The simulation complements the experimental results obtained by Kammeyer et al.[5,6] providing useful insights to in situ calibration uncertainty of PSP.

Simulated In Situ PSP Calibration in Subsonic Joukowsky Airfoil Flows

Hypothetical PSP measurements on a Joukowsky airfoil in subsonic flows are considered to estimate in situ PSP calibration uncertainty. The airfoil and incompressible potential flows around it are generated using the Joukowsky transform. The pressure coefficients on the airfoil in the corresponding subsonic compressible flows are obtained using the Kármán–Tsien rule. We consider an adiabatic model at which the adiabatic wall temperature T_{aw} is given by $T_{\text{aw}}/T_0 = [1 + r(\gamma - 1)M^2/2][1 + (\gamma - 1)M^2/2]^{-1}$. The recovery factor is $r = 0.843$ for a laminar boundary layer on the airfoil. Assuming that the reference temperature T_{ref} in the wind-off case equals to the total temperature of the flow $T_0 = 293$ K, we can calculate the temperature difference $\Delta T = T_{\text{aw}} - T_{\text{ref}}$ between the wind-on and wind-off cases. Figure 1 shows typical distributions of the pressure coefficient C_p and adiabatic wall temperature T_{aw} on a Joukowsky airfoil at AOA = 5 deg and Mach 0.4. The airfoil has a 25% thickness and 2% camber relative to the chord.

In an object–space coordinate system whose origin is located at the leading edge of the airfoil, four light sources for illuminating PSP are placed at the locations $\boldsymbol{X}_{s1} = (-\bar{c}, 3\bar{c})$, $\boldsymbol{X}_{s2} = (2\bar{c}, 3\bar{c})$, $\boldsymbol{X}_{s3} = (-\bar{c}, -3\bar{c})$, and $\boldsymbol{X}_{s4} = (2\bar{c}, -3\bar{c})$, where $\bar{c}$ is the chord of the airfoil. When a light is modeled as a point light source with unit strength, distributions of the illumination radiance on the upper and lower surfaces of the airfoil are

$$L_{\text{up}} = |\boldsymbol{X}_{\text{up}} - \boldsymbol{X}_{s1}|^{-2} + |\boldsymbol{X}_{\text{up}} - \boldsymbol{X}_{s2}|^{-2}$$
$$L_{\text{low}} = |\boldsymbol{X}_{\text{low}} - \boldsymbol{X}_{s3}|^{-2} + |\boldsymbol{X}_{\text{low}} - \boldsymbol{X}_{s4}|^{-2} \tag{2}$$

where $\boldsymbol{X}_{\text{up}}$ and $\boldsymbol{X}_{\text{low}}$ are the coordinates of the upper and lower surfaces of the airfoil, respectively. Two cameras, viewing the upper

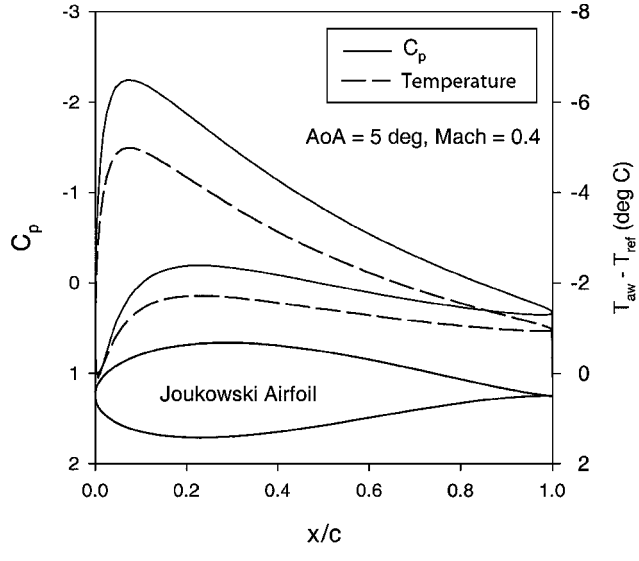

Fig. 1 Typical distributions of the pressure coefficient C_p and the adiabatic wall temperature T_{aw} on a Joukowski airfoil.

Received 5 December 2002; revision received 5 June 2003; accepted for publication 9 June 2003. This material is declared a work of the U.S. Government and is not subject to copyright protection in the United States. Copies of this paper may be made for personal or internal use, on condition that the copier pay the $10.00 per-copy fee to the Copyright Clearance Center, Inc., 222 Rosewood Drive, Danvers, MA 01923; include the code 0001-1452/03 $10.00 in correspondence with the CCC.

*Research Scientist, Aerodynamics, Aerothermodynamics and Acoustics Competency, Mail Stop 238; t.liu@larc.nasa.gov. Member AIAA.

†Professor, School of Aeronautics and Astronautics. Member AIAA.